Two-pion decays of mesons and confinement singularities

A.V. Anisovich, V.V. Anisovich, M.A. Matveev, V.A. Nikonov, J. Nyiri, and A.V. Sarantsev

March 3, 2009

Abstract

We consider the two-pion decay of the ρ-meson, the ${}^3S_1 q\bar{q}$-state of the constituent quarks – the decay being determined by the transition $q\bar{q} \to \pi\pi$ contains information about confinement interactions. One can specify in this decay two types of transitions: (**i**) the bremsstrahlung radiation of a pion $q \to q + \pi$ (or $\bar{q} \to \bar{q} + \pi$) with the subsequent fusion $q\bar{q} \to \pi$, and (**ii**) the direct transition $q\bar{q} \to \pi\pi$. We demonstrate how in the amplitudes of the corresponding transitions the quark singularities have to disappear, *i.e.* what is the way the quark confinement at relatively short distances can be realized. We calculate and estimate the contributions of processes with bremsstrahlung radiation of the pion and of the direct transition $q\bar{q} \to \pi\pi$. The estimates demonstrate that the processes involving the direct transition $q\bar{q} \to \pi\pi$ are necessary, but they cannot be determined unambiguously by the decay $\rho(775) \to \pi\pi$. We conclude that for the determination of the $q\bar{q} \to \pi\pi$ transition more complete data on the resonance decays into the $\pi\pi$ channels are required than those available at the moment.

1 Introduction

We make an attempt to restore the structure of hadrons (beginning, naturally, with the simplest ones – the light mesons) using notions like constituent quarks and effective (massive) gluons. So, we are working with effective particles and build effective interactions and effective Hamiltonians which can give an adequate description of the region of soft interactions of quarks and gluons (see [1], Chapters 9 and 10).

Recently we succeeded in constructing spectral integral equations for single-component quark-antiquark systems ($b\bar{b}$, $c\bar{c}$ [2, 3, 4] and light quark $q\bar{q}$ states with isospin $I = 1$ or quarkonium type ones like ϕ and ω [5]). We found interactions describing both the levels of these states and their radiative decays (see also [1]).

Considering mesons consisting of light quarks [5], we obtained series of radially excited states. These states form with a good accuracy linear trajectories with a universal slope on the (n, M^2)-planes, where M^2 and n are masses squared and radial quantum numbers, respectively. The systematization of meson states on (n, M^2) planes leads to a good agreement with the data [6]. Examples for states lying on linear trajectories are [$\rho(775)$, $\rho(1460)$, $\rho(1870)$, $\rho(2110)$], [$\omega(780)$, $\omega(1430)$, $\omega(1830)$, $\omega(2205)$], [$\pi(140)$, $\pi(1300)$, $\pi(1800)$, $\pi(2070)$, $\pi(2360)$] and many others (see [1] for more detail).

In the present paper we investigate hadronic decays of mesons. We start with the simplest one, $\rho \to \pi\pi$. Considering simultaneously the decays of the ${}^3S_1 q\bar{q}$ mesons, namely $\omega \to \gamma\pi$, $\rho \to \gamma\pi$ and $\rho \to \pi\pi$, we have the possibility to study the confinement singularities owing to quark exchange (the Gribov confinement singularity).

In the radiative decay reactions we face two mechanisms:
(i) a bremsstrahlung emission of a photon $q \to \gamma + q$ with a subsequent transition $q\bar{q} \to \pi$ and
(ii) a bremsstrahlung-type emission of a pion $q \to \pi + q$ with a subsequent annihilation $q\bar{q} \to \gamma$.

In the $\rho \to \pi\pi$ reaction,
(i) along with the emission of a pion $q \to \pi + q$ and the subsequent transition $q\bar{q} \to \pi$,
(ii) we observe a decay caused by Gribov's confinement mechanism.
We see that the $q\bar{q} \to \pi\pi$ transition is necessary for the description of the $\rho(775) \to \pi\pi$ decay width. However, the structure of the $q\bar{q} \to \pi\pi$ amplitude itself is not determined unambiguously, there remains a freedom of choice for the form of the singularity. We consider here some possible versions. Doing so, on the basis of experimental data for $\rho(775) \to \pi\pi$ we estimate the contribution of the amplitude $q\bar{q} \to \pi\pi$ in different versions of the interaction.

In order to convince ourselves that the decay amplitude $\rho(775) \to \pi\pi$ does not contain quark singularities in any of the considered versions of the $(q\bar{q} \to \pi\pi)$-interaction (*i.e.* in all these cases the quarks are confined), we investigate the two-channel spectral equation for the ρ-meson, taking into account the $q\bar{q}$ and $\pi\pi$ channels. Supposing that the non-resonance low-energy $\pi\pi$-interaction is small, we give a solution for the two-channel spectral integral equation. As it turns out, in this case the ρ-meson propagator obtains a self-energy part $[M_\rho^2 - s]^{-1} \to [M_\rho^2 - s - B(s)]^{-1}$, where $B(s)$ is the amplitude of the $\rho(775) \to q\bar{q} \to \pi\pi \to q\bar{q} \to \rho(775)$ transition. Our calculations show explicitly that the self-energy amplitude $B(s)$ does not contain threshold singularities (and imaginary parts) related to the $q\bar{q}$-channels; in other words, it describes confined quarks. It can be seen also that the quark confinement is due to the strong singularities in the $q\bar{q} \to q\bar{q}$ - singularity channel, which create the $V_{confinement}(r) \sim b\,r$ barrier [1, 5]. However - and this can also be seen explicitly - the $q\bar{q} \to \pi\pi$ transition plays an essential role in confining the quarks. If it were not present, the bremsstrahlung emission of pions would destroy the $\rho(775)$ meson quickly, giving $\Gamma_{\rho(775)\to\pi\pi}(bremsstrahlung\,emission\,of\,pion) \simeq 2000$ MeV.

The structure of the paper is as follows. In the Introduction we provide a short description of those basic statements which we assume to be known (see [1]) and from which we start our investigations of the $\rho \to \pi\pi$ reaction. In Section 2 we calculate diagrams with bremsstrahlung emissions of pions. Then, in Section 3, we discuss the confinement singularities and calculate the triangle diagram owing to the direct production process $q\bar{q} \to \pi$. In Section 4 we discuss two-channel ($q\bar{q}$ and $\pi\pi$) equations for ρ-meson states as well as the self-energy part in by the transition $\rho(775) \to q\bar{q} \to \pi\pi \to q\bar{q} \to \rho(775)$. Results of the calculations are summarized in the Conclusion.

1.1 Spectral integral equation and confinement singularity

The linearity of the trajectories in the (n, M^2) planes (experimentally – up to large n values, $n \leq 7$) provides us the t-channel singularity $V_{conf} \sim 1/q^4$ or, in coordinate representation, $V_{conf} \sim r$. In the coordinate representation the confinement interaction can be written in the

following potential form [5] (see Fig. 1):

$$V_{conf} = (I \otimes I)\, b_S\, r + (\gamma_\mu \otimes \gamma_\mu)\, b_V\, r \ , \qquad (1)$$
$$b_S \simeq -b_V \simeq 0.15 \ \mathrm{GeV}^{-2} \ .$$

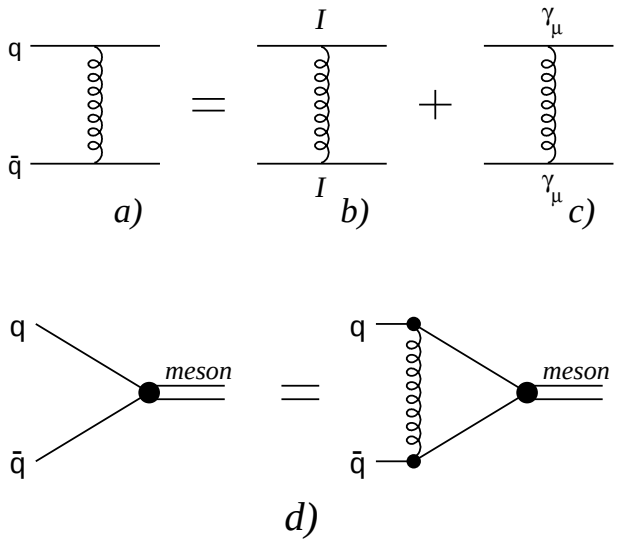

Figure 1: Diagrams for confinement singularities $1/q^4$: scalar (b) and vector (c) exchanges in the t-channel. (d) Graphical representation of the spectral integral equation for the meson-$q\bar{q}$ vertex with t-channel confinement interaction.

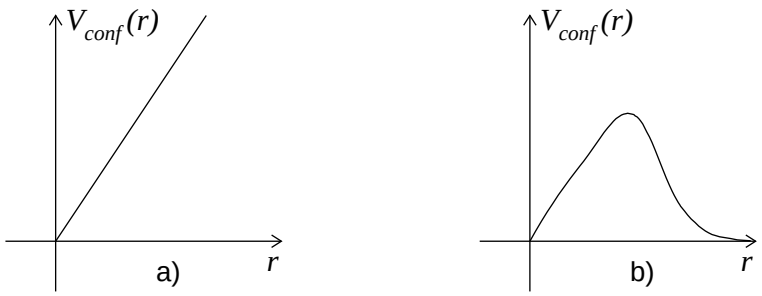

Figure 2: Confinement singularity in coordinate representation a) without cut-off: $V_{conf}(r) \sim b\, r$, and b) introducing a cut-off: $V_{conf}(r) \sim b\, r e^{-\mu r}$.

The position of $q\bar{q}$ levels and data on radial decays tell us that singular t-channel exchanges are necessary both in the scalar $(I \otimes I)$ and the vector $(\gamma_\mu \otimes \gamma_\mu)$ channels. The t-channel exchange interactions (1) can take place both in white and colour states, $\mathbf{c} = \mathbf{1} + \mathbf{8}$ though, of course, the colour-octet interaction plays a dominant role.

The spectral integral equation for the meson-$q\bar{q}$ vertex (or for the $q\bar{q}$ wave function of the meson, see Fig. 1d) was solved by introducing a cut-off into the interaction (1): $r \to r e^{-\mu r}$, see Fig. 2. The cut-off parameter is small: $\mu \sim 1 - 10$ MeV; if μ is changing in this interval, the $q\bar{q}$-levels with $n \leq 7$ remain practically the same.

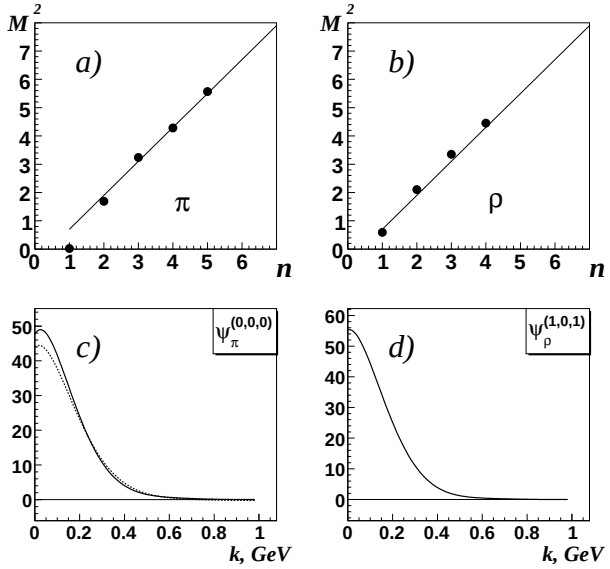

Figure 3: a) The π-trajectory in the (n, M^2) - plane; b) ρ/ω - trajectory; c) wave function of the π-meson obtained in the spectral integral equation [5] (solid line) and in the phenomenological fit [7] (dotted line).

In [3, 4, 5] the spectral integral equations were solved in momentum representation – this is natural, since we used dispersion integration technics (see the discussion in [1]). In this representation the interaction is re-written as

$$re^{-\mu r} \to 8\pi \left(\frac{4\mu^2}{(\mu^2 - t_\perp)^3} - \frac{1}{(\mu^2 - t_\perp)^2} \right). \tag{2}$$

In general, having in mind that in the framework of spectral integration (as in dispersion technics) the total energy is not conserved, we have to write

$$t_\perp = (k_1^\perp - k_1'^\perp)_\mu (-k_2^\perp + k_2'^\perp)_\mu \tag{3}$$

for the momentum transferred, where k_1 and k_2 are the momenta of the initial quark and antiquark, while k_1' and k_2' are those after the interaction. The index $\perp$ means that we use components perpendicular to the total momentum p for the initial state and to p' for the final state:

$$k_{i\,\mu}^\perp = g_{\mu\nu}^{\perp p} k_{i\,\nu} \ , \quad g_{\mu\nu}^{\perp p} = g_{\mu\nu} - \frac{p_\mu p_\nu}{p^2} \ , \quad p = k_1 + k_2 \ , \quad p^2 = s \, , \tag{4}$$

$$k_{i\,\mu}'^\perp = g_{\mu\nu}^{\perp p'} k_{i\,\nu}' \ , \quad g_{\mu\nu}^{\perp p'} = g_{\mu\nu} - \frac{p_\mu' p_\nu'}{p'^2} \ , \quad p' = k_1' + k_2' \, , \quad p'^2 = s' \ .$$

For quarks with equal masses we write $t_\perp = (k_1^\perp - k_1'^\perp)^2 = (-k_2^\perp + k_2'^\perp)^2$. If energies in the initial and final states are equal ($s = s'$), we have $t^\perp = -\vec{q}^{\,2}$, and the t-channel singular term in the right-hand side of (2) is equivalent to the interaction $r\, e^{-\mu r}$ after the Fourier transform. In the general case we can write

$$r^N e^{-\mu r} = \int \frac{d^3 q}{(2\pi)^3} e^{-i\vec{q}\vec{r}} I_N(t_\perp) \ , \tag{5}$$

$$I_N(t_\perp) = \frac{4\pi (N+1)!}{(\mu^2 - t_\perp)^{N+2}} \sum_{n=0}^{N+1} \left(\mu + \sqrt{t_\perp} \right)^{N+1-n} \left(\mu - \sqrt{t_\perp} \right)^n \ .$$

In Fig. 3a,b the (n, M^2)-trajectories for π, ρ and ω mesons are shown (the ρ and ω trajectories coincide with a good accuracy). As we see, the π meson mass ($\sim 140\,\mathrm{MeV}$) sticks out on the linear trajectory. This happens due to an instanton-induced interaction. In Fig. 3c,d one can see the pion and ρ/ω wave functions. At $k > 0.15$ keV the pion wave function obtained in the spectral integral equation coincides with a good accuracy with the phenomenological wave function [7], which was found by the fit of the pion form factor; small deviations ($\sim 10\%$) are observed in the region of very small k values.

1.2 Instability of $q\bar{q}$ levels - quark deconfinement

All quark-antiquark levels except for the lowest $J^P = 0^-$ states decay into hadron states, *i.e.* quarks become deconfined. New quark pairs are produced and, as a result, the initial quarks leave the confinement trap, finding a suitable partner among the newly born quarks to form white hadrons in the final state.

Such general considerations about quark deconfinement were expressed many times and discussed long ago (see, for example, [8, 9, 10] and references therein). However, it is the details of the mechanism what really matters, and they were not presented. A detailed scheme for the quark deconfinement was suggested in [11] – in the main points the present investigations of the deconfinement process follow these ideas.

1.2.1 Instability of $q\bar{q}$ levels owing to radiative decays.

In the calculations [5] the levels are instable, as can be seen from Fig. 2b. But this is, so to say, a "technical" instability, owing to the method of calculation. It is convenient to discuss the physical mechanism of the instability, considering first the radiative decays.

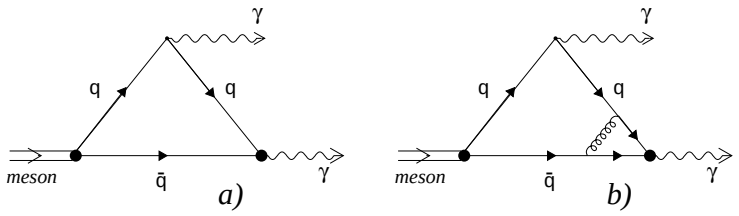

Figure 4: Quark model mechanism for the $meson \to \gamma\gamma$ decay: a) bremsstrahlung photon radiation and the subsequent annihilation process $q\bar{q} \to \gamma$. The annihilation block includes quark interactions, among others long range ones (b).

(i) $meson \to \gamma\gamma$ **decays**

Considering this decay in the framework of the quark model, we face two relevant mechanisms: the bremsstrahlung radiation of a photon by a quark or antiquark, and the subsequent annihilation $q\bar{q} \to \gamma$. In Fig. 4 the bremsstrahlung radiation by a quark is shown only, but, naturally, there is a similar process of bremsstrahlung radiation by an antiquark. In the annihilation vertex, quark interactions (including the confinement interaction) are also present. In the considered process the quarks do not leave the quark trap, but, on the other hand, mesons are also not flying away. So, let us consider a different decay process in which a meson (a pion) leaves the confinement region.

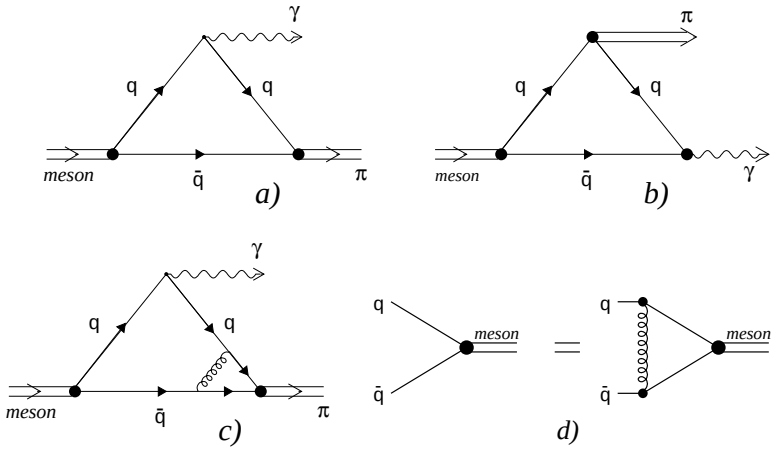

Figure 5: Emission of a photon (a) and a pion (b) in the $\rho, \omega \to \gamma\pi$ processes. c) The annihilation block $q\bar{q} \to \pi$ includes quark interactions similar to that in Fig. 4b. d) Spectral integral equation which determines the $q\bar{q} \to \pi$ transition block.

(ii) $meson \to \gamma\pi$ **decays**

This decay consists of two types of processes: the bremsstrahlung of a photon with the subsequent $q\bar{q} \to \pi$ transition (Fig. 5a) and the bremsstrahlung-type pion radiation (the pion has a small mass) with the subsequent $q\bar{q} \to \gamma$ annihilation (Fig. 5b) (as in the previous case, we show here the radiation by a quark only). In Fig. 5c we emphasize that in the annihilation block $q\bar{q} \to \pi$ the quark-antiquark interactions are included. It is just due to these interactions that the $q\bar{q} \to \pi$ block satisfies the spectral integral equation [5] (see Fig. 5d); the spectral integral equation contains, naturally, the confinement interaction.

Hence, in both processes, $meson \to \gamma\gamma$ (Fig. 4) and $meson \to \gamma\pi$ (Fig. 5), the confinement interaction (or the confinement singularity) plays a relevant role at the last stage: in the $q\bar{q}$ annihilation and in the formation of a pion.

(iii) The $\rho \to \pi\pi$ **decay**

In hadronic decays the confinement interaction plays, of course, a decisive role but the bremsstrahlung-type emission of pions may also be important if there are pions among the particles of the outgoing state.

The decay processes $\rho \to \pi\pi$ (to be definite, we consider $\rho^+ \to \pi^0\pi^+$) are demonstrated in Fig. 6. While the processes Fig. 6a,b do not differ essentially from those shown in Fig. 5a,b for $\rho \to \gamma\pi$, the process Fig. 6c is principally different. In the processes in Fig. 5a,b and Fig. 6a,b one of the particles (the photon or the pion) is emitted by a constituent quark when it is inside a "bag" (in the region where colour quarks can exist). Further, two quarks form a particle: a pion (Fig. 5a and 6a,b) or a photon (Fig. 5b) – obviously, with the participation of the confinement interaction (see Figs. 4b and 5c). In the process shown in Fig. 6c there is a transition of $q\bar{q}$ into two mesons, $q\bar{q} \to \pi\pi$. The confinement singularity, but with fermion quantum numbers, has to play a crucial role here. As it was stressed by Gribov [11], the corresponding forces must be long-range ones, *i.e.* the effective mass of the exchange fermion state has to be small on the hadron scale.

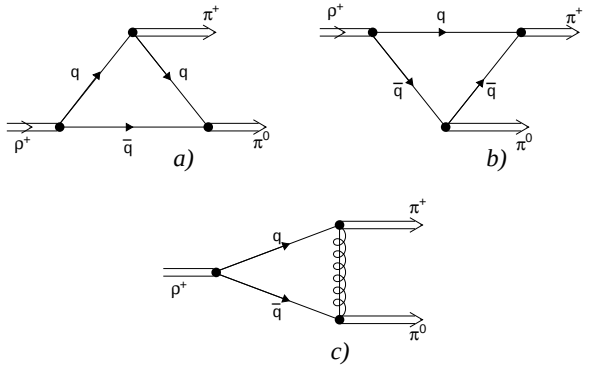

Figure 6: The $\rho^+ \to \pi^+\pi^0$ process: a,b) with a bremsstrahlung-type pion emission and c) with the $q\bar{q} \to \pi\pi$ transition, realized owing to the t-channel confinement singularity with fermion quantum numbers.

2 Diagrams with bremsstrahlung pion emission

We have two diagrams with bremsstrahlung pion emission, they are presented in Fig. 7. Let us denote the amplitudes in Fig. 7 as follows:

$$A_\nu^{\rho^+\to\pi^+\pi^0}(\text{emission}) = \mathrm{p}_{\pi^+\nu}^{\perp \mathrm{p}} \left[\mathrm{A}(\triangle_0^+) + \mathrm{A}(\triangledown_0^+) + \mathrm{A}(\triangle_+^0) + \mathrm{A}(\triangledown_+^0)\right] \ . \tag{6}$$

In the triangle diagrams of Fig. 7 quarks are moving clockwise.

2.1 Calculation of the diagrams of Fig. 7

Let us first calculate the diagrams in Fig. 7a,b. In the framework of spectral integration technics they read:

$$A(\triangle_0^+) = \zeta(\triangle_0^+) \int\limits_{4m^2}^{\infty} \frac{ds}{\pi}\frac{ds'}{\pi}\psi_\rho(s) d\Phi_\triangle(P,P';k_1,k_1',k_2) g_\pi S_{\triangle_0^+}(s,s',M_\pi^2)\psi_\pi(s'),$$
$$A(\triangledown_0^+) = \zeta(\triangledown_0^+) \int\limits_{4m^2}^{\infty} \frac{ds}{\pi}\frac{ds'}{\pi}\psi_\rho(s) d\Phi_\triangledown(P,P';k_2,k_2',k_1) g_\pi S_{\triangledown_0^+}(s,s',M_\pi^2)\psi_\pi(s'). \tag{7}$$

Here $\zeta(\triangle_0^+)$ and $\zeta(\triangle_0^+)$ are the isotopic factors, $\zeta(\triangle_0^+) = \zeta(\triangle_0^+) = -1/\sqrt{2}$ (we mean $\pi^0 = (u\bar{u} - d\bar{d})/\sqrt{2}$; the phase volume of the triangle diagram can be written in the standard way in the double spectral integral:

$$d\Phi_\triangle(P,P';k_1,k_1',k_2)\frac{1}{64\pi}\frac{d^3k_1}{k_{10}}\frac{d^3k_2}{k_{20}}\frac{d^3k_1'}{k_{10}'}\delta^{(4)}(P-k_1-k_2)\delta^{(4)}(P'-k_1'-k_2),$$
$$d\Phi_\triangledown(P,P';k_2,k_2',k_1)\frac{1}{64\pi}\frac{d^3k_2}{k_{20}}\frac{d^3k_1}{k_{10}}\frac{d^3k_2'}{k_{20}'}\delta^{(4)}(P-k_1-k_2)\delta^{(4)}(P'-k_2'-k_1). \tag{8}$$

The spin factors $S_{\triangle_0^+}(s,s',\mu_\pi^2)$ and $S_{\triangledown_0^+}(s,s',M_\pi^2)$ are calculated by considering the traces corresponding to the quark loops of Fig. 7a:

$$-Sp[(\hat{k}_1+m)i\gamma_5(\hat{k}_1'+m)i\gamma_5(-\hat{k}_2+m)\gamma_\nu^{\perp P}] = (-P_\nu'^{\perp P})S_{\triangle_0^+}(s,s',M_\pi^2),$$
$$-Sp[(\hat{k}_1+m)i\gamma_5(-\hat{k}_2'+m)i\gamma_5(-\hat{k}_2+m)\gamma_\nu^{\perp P}] = (-P_\nu'^{\perp P})S_{\triangledown_0^+}(s,s',M_\pi^2). \tag{9}$$

We have

$$S_{\triangle_0^+}(s,s',M_\pi^2)=S_{\triangledown_0^+}(s,s',M_\pi^2)=\frac{8M_\pi^2ss'}{-(s-s')^2+2M_\pi^2(s+s')-M_\pi^4}=\frac{-8M_\pi^2ss'}{\lambda(s,s',M_\pi^2)}. \qquad (10)$$

Calculating the spin factor, we gave the definition (6) and used the relation $p^{\perp p}_{\pi^0\,\nu}=-p^{\perp p}_{\pi^+\,\nu}$.

In (7) the pion emission constant g_π is present. It was determined from the reactions $\rho\to\gamma\pi$ and $\omega\to\gamma\pi$ [12]. We have two solutions:

$$\begin{aligned}\text{Solution I} \quad &: \qquad g_\pi=16.7\pm0.3\ {}^{+0.1}_{-2.3}\ ,\\ \text{Solution II} \quad &: \qquad g_\pi=-3.0\pm0.3\ {}^{+2.1}_{-0.1}\ . \end{aligned} \qquad (11)$$

In Eq. (11) we have included systematical errors ($(+0.1/-2.3)$ for Solution I and $(+2.1/-0.1)$ for Solution II) which are caused by the uncertainties of the fit of $q\bar{q}$ wave functions in the spectral integral equation.

So, we have regions of positive and negative g_π. However, one should take into account that the sign of g_π in (11) is rather conventional: it depends on the signs of the wave functions of photons and mesons involved in the calculation. Because of that, to be precise, we should state that for g_π we determine absolute values only.

Solution I gives us the value of the of pion–nucleon coupling; recall that it is determined as a factor in the phenomenological Lagrangian: $g_{\pi NN}\Big(\bar{\psi}'_N(\vec{\tau}\vec{\varphi}_\pi)i\gamma_5\psi_N\Big)$. It is in agreement with the results for pion–nucleon scattering $g^2_{\pi NN}/4\pi\simeq14$ [13, 14, 15].

The amplitude $A(\triangle_0^+)$ can be calculated directly by (10) if $M_\pi^2<0$, *i.e.* in the non-physical pion mass region. This is, however, not a serious problem: one can carry out a few calculations at $M_\pi^2<0$ close to $M_\pi^2=0$, and after that extrapolate, by making use, *e.g.*, of the formula

$$A(\triangle_0^+,\ M_\pi^2)\simeq a+bM_\pi^2+cM_\pi^4 \qquad (12)$$

to arrive at $M_\pi^2=0.02$ GeV^2 (or, $M_\pi=140$ MeV).

Hence, let us write (7) in the form:

$$\begin{aligned}A(\triangle_0^+)=&\zeta(\triangle_0^+)\int\limits_{4m^2}^{\infty}\frac{dsds'}{\pi^2}\psi_\rho(s)\frac{\Theta(-M_\pi^2ss'-M_\pi^2\lambda(s,s',M_\pi^2))}{16\sqrt{\lambda(s,s',M_\pi^2)}}g_\pi S_{\triangle_0^+}(s,s',M_\pi^2)\psi_\pi(s'),\\ A(\triangle_0^+,M_\pi^2=0)=&\zeta(\triangle_0^+)\int\limits_{4m^2}^{\infty}\frac{ds}{16\pi^2}\psi_\rho(s)g_\pi\psi_\pi(s)4s\sqrt{1-\frac{4m^2}{s}}. \end{aligned} \qquad (13)$$

Similar calculations demonstrate that the contributions of the processes of Fig. 7 are equal:

$$A(\triangle_0^+)=A(\triangledown_0^+)=A(\triangle_+^0)=A(\triangledown_+^0), \qquad (14)$$

2.2 Results of the calculations of the bremsstrahlung emission width

The width of the $\rho\to\pi\pi$ decay is determined as follows:

$$M_\rho\Gamma^{(\text{emission})}_{\rho\to\pi\pi} \ = \ \int d\Phi_2(p;p_{\pi^0},p_{\pi^+})\frac{1}{3}\sum_\nu\ \left|p^{\perp p}_{\pi^+\nu}\cdot4A\left(\triangle^{\pi^+}_{\pi^0}\right)\right|^2$$

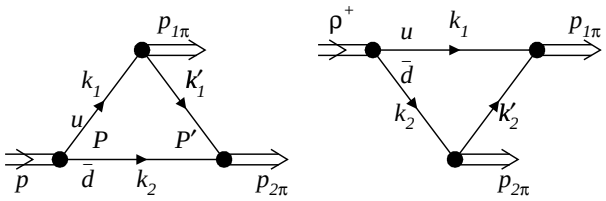

Figure 7: Processes of pion emission by quarks inside the confinement region, with the subsequent $q\bar{q} \to \pi$ annihilation.

$$= \frac{1}{3}\frac{1}{16\pi}\sqrt{1-\frac{4M_\pi^2}{M_\rho^2}}\left(\frac{M_\rho^2}{4}-M_\pi^2\right)16\left|A\left(\triangle_{\pi^0}^{\pi^+}\right)\right|^2 \tag{15}$$

The factor 1/3 is the consequence of averaging over the ρ meson spin. Recall that $p^2 = M_\rho^2$ and $|p_{\pi^+\nu}^{\perp p}|^2 = M_\rho^2/4 - M_\pi^2$.

The processes containing only pion emission give widths essentially larger than those observed in experiments. For Solution I, Eq. (11), we obtain:
$\Gamma_{\rho(775)\to\pi\pi}(bremsstrahlung\, emission\, of\, pion) \simeq 2000$ MeV.
This means that the pion bremsstrahlung amplitudes are reconciled with the amplitude of the direct transition $q\bar{q} \to \pi\pi$, Fig. 6c.

3 The confinement singularity and the direct transition process $q\bar{q} \to \pi\pi$, Fig. 6c

Considering the confinement singularity which is the attribute of the direct $q\bar{q} \to \pi\pi$ transition, Fig. 6c, we make use of the results obtained in [5] when searching for $q\bar{q}$-levels in the framework of the spectral integral approach.

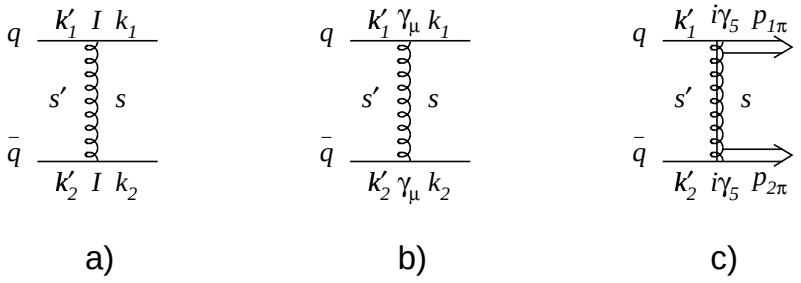

Figure 8: Amplitude with confinement singularities: a) scalar exchange, b) vector exchange, c) quark (fermionic) exchange.

3.1 Confinement singularities

We discuss here three types of amplitudes with t-channel confinement singularities, they are presented in Fig. 8. In Figs. 8a and 8b we show t-channel singularities for scalar and vector exchanges between quark and antiquark; they were used in [5] when obtaining the $q\bar{q}$-levels (see also Fig. 5d where the corresponding equation is shown). In Fig. 8c the amplitude with a confinement singularity is drawn for the $q\bar{q} \to \pi_1\pi_2$ transition.

Introducing the momenta of quarks and antiquarks we stress that the total energies are not conserved in the spectral integrals (just as in dispersion relations). Hence, in the general case $s \neq s'$.

3.1.1 Confinement singularities in $q\bar{q}$ interaction

We write the amplitudes of Fig. 8a,b in the following form [5]:

$$\begin{aligned} &\mathrm{S-exchange}: \quad \Big(\bar{\Psi}(k_1')\, I\, \Psi(k_1)\Big)\, G_S(t_\perp)\, I_1^{(\mu\to 0)}(t_\perp)\, \Big(\bar{\Psi}(-k_2)\, I\, \Psi(k_2')\Big)\,, \\ &\mathrm{V-exchange}: \quad -\Big(\bar{\Psi}(k_1')\, \gamma_\mu\, \Psi(k_1)\Big)\, G_V(t_\perp)\, I_1^{(\mu\to 0)}(t_\perp)\, \Big(\bar{\Psi}(-k_2)\, \gamma_\mu\, \Psi(k_2')\Big)\,. \end{aligned} \tag{16}$$

The singular block, $I_1^{(\mu\to 0)}(t_\perp)$, is given in (5), where $t_\perp = (q^\perp)^2 = (k_1^{\perp p} - k_1'^{\perp p'})^2$ with $p = k_1 + k_2$ and $p' = k_1' + k_2'$ ($p^2 = s$, $p'^2 = s'$); the transverse components are defined as $k_{1\alpha}^{\perp p} = g_{\alpha\beta}^{\perp p} k_{1\beta}$, $g_{\alpha\beta}^{\perp p} = g_{\alpha\beta} - p_\alpha p_\beta/p^2$ and $k_{1\alpha}'^{\perp p'} = g_{\alpha\beta}^{\perp p'} k_{1\beta}'$, $g_{\alpha\beta}^{\perp p'} = g_{\alpha\beta} - p_\alpha' p_\beta'/p'^2$.

In [5] we have used several singular terms corresponding to the expansion:

$$G_S(t_\perp) = G_S(0) + G_S(1)\, t_\perp + G_S(2) t_\perp^2, \quad G_V(t_\perp) = G_V(0) + G_V(1)\, t_\perp + G_V(2) t_\perp^2. \tag{17}$$

We use (16) as a pattern in writing the amplitude for the $q\bar{q} \to \pi\pi$ transition.

3.1.2 Confinement singularities in $q\bar{q} \to \pi\pi$ transition

The quark-exchange singularity of Fig. 8c reads:

$$\phi_{\pi(1)}^* \phi_{\pi(2)}^* \left(\bar{\Psi}(-k_2')\, i\gamma_5 \sum_a \Psi_{conf}^{(a)}(q^\perp) G_{q\bar{q}\to\pi\pi}(t_\perp)\, I_N^{(\mu\to 0)}(t_\perp)\, \bar{\Psi}_{conf}^{(a)}(q^\perp)\, i\gamma_5 \Psi(k_1') \right) \tag{18}$$

In Fig. 8c we have $q^\perp = k_1'^{\perp p'} - p_{\pi 1}^{\perp p}$ with $p_{\pi 1\alpha}^{\perp p} = g_{\alpha\beta}^{\perp p} p_{\pi 1\beta}$.

Below we consider two types of the spin structure for the confinement singularity.

(i) Gribov quark-exchange interaction

Following [11], we accept that the mass of the t-channel quark state is very small. We put it to be zero. Then we write the completeness condition in a standard form:

$$\sum_a \Psi_{conf}^{(a)}(q^\perp) \bar{\Psi}_{conf}^{(a)}(q^\perp) = \hat{q}^\perp\,. \tag{19}$$

Equation (18) reads:

$$\phi_{\pi(1)}^* \phi_{\pi(2)}^* \left(\bar{\Psi}(-k_2')\, i\gamma_5 \hat{q}^\perp I_N^{(\mu\to 0)}(t_\perp) G_{q\bar{q}\to\pi\pi}(t_\perp)\, i\gamma_5 \Psi(k_1') \right). \tag{20}$$

Considering the performed here calculations as first estimations, we use interaction singularities $I_1^{(\mu\to 0)}(t_\perp)$ with $N=1,0,-1$ and constant non-singular coefficients $G_{q\bar{q}\to\pi\pi}(t_\perp)=const$:

$$G_{q\bar{q}\to\pi\pi}(t_\perp)\, I_1^{(\mu\to 0)}(t_\perp) \to \sum_{N=-1}^{1} G_{q\bar{q}\to\pi\pi}(1-N)\, I_N^{(\mu\to 0)}(t_\perp) \tag{21}$$
$$= G_{q\bar{q}\to\pi\pi}(0)\, I_1^{(\mu\to 0)}(t_\perp) + G_{q\bar{q}\to\pi\pi}(1)\, I_0^{(\mu\to 0)}(t_\perp) + G_{q\bar{q}\to\pi\pi}(2)\, I_{-1}^{(\mu\to 0)}(t_\perp).$$

Thus, we use the singularities of the same type as in the $q\bar{q}$ interaction, see (16) and (17).

(ii) Universal confinement singularity

The universality of the confinement singularity appears when the spin functions in the t-channel exchange obey the following completeness condition:

$$\sum_a \Psi^{(a)}_{conf}(q^\perp)\bar{\Psi}^{(a)}_{conf}(q^\perp) = I, \tag{22}$$

where $I=diag(1,1,1,1)$ is a unit four-dimensional matrix in the spin space. We re-write (18):

$$\phi^*_{\pi(1)}\phi^*_{\pi(2)}\left(\bar{\Psi}(-k_2')\, i\gamma_5 I_1^{(\mu\to 0)}(t_\perp)\, i\gamma_5 G_{q\bar{q}\to\pi\pi}(t_\perp)\Psi(k_1')\right) \tag{23}$$
$$= -\phi^*_{\pi(1)}\phi^*_{\pi(2)}\left(\bar{\Psi}(-k_2') I_1^{(\mu\to 0)}(t_\perp) G_{q\bar{q}\to\pi\pi}(t_\perp)\Psi(k_1')\right),$$
$$I_1^{(\mu\to 0)}(t_\perp) G_{q\bar{q}\to\pi\pi}(t_\perp) \to \sum_{N=-1}^{1} G_{q\bar{q}\to\pi\pi}(1-N)\, I_N^{(\mu\to 0)}(t_\perp).$$

Then Eq. (23) gives the singularity of the same type as in transition $q\bar{q}\to q\bar{q}$, see Eq. (16).

3.1.3 An example: expressions for $q_\perp$ and $t_\perp$ in the centre-of-mass system

To make our calculations more understandable, let us present here the expressions for $q_\perp$ and $t_\perp$ in the centre-of-mass system, taking into account that in a spectral integral the initial and final state energies are different.

The momenta in the diagrams Fig. 8a,b have the following form in the centre-of-mass frame:

$$k_1 = \left(\frac{\sqrt{s}}{2}, \vec{n}\sqrt{\frac{s}{4}-m^2}\right), \qquad k_1' = \left(\frac{\sqrt{s'}}{2}, \vec{n}'\sqrt{\frac{s'}{4}-m^2}\right), \tag{24}$$
$$k_2 = \left(\frac{\sqrt{s}}{2}, -\vec{n}\sqrt{\frac{s}{4}-m^2}\right), \qquad k_2' = \left(\frac{\sqrt{s'}}{2}, -\vec{n}'\sqrt{\frac{s'}{4}-m^2}\right).$$

In accordance with this,

$$k_1^\perp = \left(0, \vec{n}\sqrt{\frac{s}{4}-m^2}\right), \qquad k_1'^\perp = \left(0, \vec{n}'\sqrt{\frac{s'}{4}-m^2}\right), \tag{25}$$
$$k_2^\perp = \left(0, -\vec{n}\sqrt{\frac{s}{4}-m^2}\right), \qquad k_2'^\perp = \left(0, -\vec{n}'\sqrt{\frac{s'}{4}-m^2}\right),$$

and in the c.m. system we write

$$q^\perp = k_1^\perp - k_1'^\perp = -k_2^\perp + k_2'^\perp = \left(0, \vec{n}\sqrt{\frac{s}{4} - m^2} - \vec{n}'\sqrt{\frac{s'}{4} - m^2}\right). \tag{26}$$

Similarly, for the process in Fig. 8c we have:

$$\begin{aligned}
p_{1\pi} &= \left(\frac{s + M_{1\pi}^2 - M_{2\pi}^2}{2\sqrt{s}}, \quad \vec{n}_\pi\sqrt{\frac{1}{4s}\left[s - (M_{1\pi} + M_{2\pi})^2\right]\left[s - (M_{1\pi} - M_{2\pi})^2\right]}\right), \\
p_{2\pi} &= \left(\frac{s - M_{1\pi}^2 + M_{2\pi}^2}{2\sqrt{s}}, -\vec{n}_\pi\sqrt{\frac{1}{4s}\left[s - (M_{1\pi} + M_{2\pi})^2\right]\left[s - (M_{1\pi} - M_{2\pi})^2\right]}\right), \\
p_{1\pi}^\perp &= \left(0, \quad \vec{n}_\pi\sqrt{\frac{1}{4s}\left[s - (M_{1\pi} + M_{2\pi})^2\right]\left[s - (M_{1\pi} - M_{2\pi})^2\right]}\right), \\
p_{2\pi}^\perp &= \left(0, -\vec{n}_\pi\sqrt{\frac{1}{4s}\left[s - (M_{1\pi} + M_{2\pi})^2\right]\left[s - (M_{1\pi} - M_{2\pi})^2\right]}\right).
\end{aligned} \tag{27}$$

that leads to

$$q^\perp = \left(0, \vec{n}\sqrt{\frac{s}{4} - m^2} - \vec{n}_\pi\sqrt{\frac{1}{4s}\left[s - (M_{1\pi} + M_{2\pi})^2\right]\left[s - (M_{1\pi} - M_{2\pi})^2\right]}\right). \tag{28}$$

In order to preserve the possibility to generalize, we take into account in (27) and (28) that π_1 and π_2 can have different masses, respectively, $M_{1\pi}$ and $M_{2\pi}$. Below we neglect this difference and put $M_{1\pi} = M_{2\pi} \equiv M_\pi$.

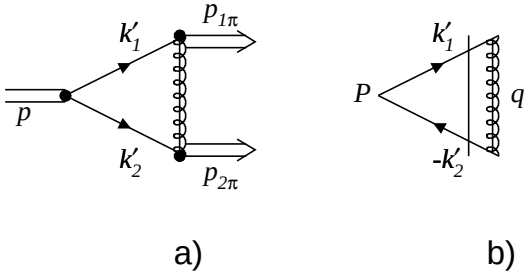

Figure 9: Triangle diagram $\rho \to \pi^+\pi^0$, and the notation of momenta in the spectral integral.

3.2 Calculation of the direct transition amplitude $\rho \to \pi\pi$ in the framework of spectral integration technics

Here we calculate amplitude of the transition Fig. 6c; the transition diagram with the notation of momenta is shown separately in Fig. 9a.

The amplitude of the $\rho^+ \to \pi^+\pi^0$ decay has the structure

$$\begin{aligned}
A_\nu\left(\sphericalangle_{\pi^0}^{\pi^+}; s, M_\rho^2\right) + A_\nu\left(\sphericalangle_{\pi^+}^{\pi^0}; s, M_\rho^2\right) &= p_{\pi^+\nu}^\perp\left[A\left(\sphericalangle_{\pi^0}^{\pi^+}; s, M_\rho^2\right) + A\left(\sphericalangle_{\pi^+}^{\pi^0}; s, M_\rho^2\right)\right] \\
&= p_{\pi^+\nu}^\perp A(\sphericalangle; s, M_\rho^2)(\text{direct transition}) .
\end{aligned} \tag{29}$$

Let us remind that $p^{\perp p}_{\pi^+\nu} = -p^{\perp p}_{\pi^0\nu}$ and $p = p_{\pi^+} + p_{\pi^0}$. In spectral integrals the energy is not conserved, so $s \neq M_\rho^2$. For physical amplitudes $s = M_\rho^2$.

To be definite, let us consider $A_\nu\left(\sphericalangle^{\pi^+}_{\pi^0}; s, M_\rho^2\right)$.

3.2.1 Gribov quark-exchange interaction

For the Gribov quark-exchange interaction the amplitude reads:

$$A_\nu\left(\sphericalangle^{\pi^+}_{\pi^0}; s, M_\rho^2\right) = \int\limits_{4m^2}^{\infty} \frac{ds'}{\pi}\Psi_\rho(s')d\Phi_2(p'; k_1', k_2') \tag{30}$$
$$\times(-)Sp\Big[(\hat{k}_1' + m)\hat{q}^\perp G_{q\bar{q}\to\pi\pi}(t_\perp) I_N^{(\mu\to 0)}(t_\perp)(-k_2' + m)\gamma_\nu^{\perp p'}\Big].$$

Here the ρ-meson wave function is the ratio of the vertex of $\rho \to \pi\pi$, $G_{\rho\to q\bar{q}}(s')$ and the dispersion integral denominator $\Psi_\rho(s) = G_{\rho\to q\bar{q}}(s')/(s' - M_\rho^2)$, while the two-particle phase volume is written in a standard form:

$$d\Phi_2(p'; k_1', k_2') = \frac{1}{2}(2\pi)^4 \frac{d^3k_1'}{2k_{10}'(2\pi)^3}\frac{d^3k_2'}{2k_{20}'(2\pi)^3}\delta^4(p' - k_1' - k_2') \tag{31}$$

with $p'^2 = s'$, $k_1'^2 = m^2$, $k_2'^2 = m^2$. The transverse momentum is $q^\perp = k_1'^\perp - p^\perp_{\pi^+}$, or, in the c.m. system (see section 2.1.3): $q^\perp = (0, \vec{n}'\sqrt{s'/4 - m^2} - \vec{n}_\pi\sqrt{s/4 - M_\pi^2})$.

To extract the invariant part of the amplitude $p^\perp_{\pi^+\nu} A\left(\sphericalangle^{\pi^+}_{\pi^0}; s, M_\rho^2\right)$, we write:

$$A\left(\sphericalangle^{\pi^+}_{\pi^0}; s, M_\rho^2\right) = \int\limits_{4m^2}^{\infty} \frac{ds'}{\pi}\Psi_\rho(s')d\Phi_2(p'; k_1', k_2') \tag{32}$$
$$\times(-)Sp\Big[(\hat{k}_1' + m)\hat{q}^\perp G_{q\bar{q}\to\pi\pi}(t_\perp) I_1^{(\mu\to 0)}(t_\perp)(-\hat{k}_2' + m)\gamma_\nu^{\perp p'}\Big]\frac{p^{\perp p}_{\pi^+\nu}}{(p^{\perp p}_{\pi^+\nu'})^2}$$
$$= \int\limits_{4m^2}^{\infty} \frac{ds'}{\pi}\Psi_\rho(s')d\Phi_2(p'; k_1', k_2')(-8)\frac{4(k_1'q^\perp)(k_1'p_{1\pi}) + s'(q^\perp p_{1\pi})}{4M_\pi^2 - s},$$

where $(k_1'p_{1\pi}) = -z'\sqrt{s'/4 - m^2}\sqrt{s/4 - M_\pi^2}$, $\quad (k_1'q^\perp) = -s'/4 + m^2 + z'\sqrt{s'/4 - m^2}\sqrt{s/4 - M_\pi^2}$ and $(q^\perp p_{1\pi}) = s/4 - M_\pi^2 - z'\sqrt{s'/4 - m^2}\sqrt{s/4 - M_\pi^2}$.

It is easy to see that in (29) we have $A\left(\sphericalangle^{\pi^+}_{\pi^0}; s, M_\rho^2\right) = A\left(\sphericalangle^{\pi^0}_{\pi^+}; s, M_\rho^2\right)$ and, hence,

$$p^\perp_{\pi^+\nu} A(\sphericalangle; s, M_\rho^2) = p^\perp_{\pi^+\nu} \cdot 2A\left(\sphericalangle^{\pi^+}_{\pi^0}; s, M_\rho^2\right). \tag{33}$$

Let us emphasize once more that the amplitude $A_\nu\left(\sphericalangle^{\pi^+}_{\pi^0}; s, M_\rho^2\right)$ is an auxiliary one, the physical amplitude requires $s \to M_\rho^2$:

$$\Big[A_\nu\left(\sphericalangle^{\pi^+}_{\pi^0}; s, M_\rho^2\right)\Big]_{s\to M_\rho^2} = A_\nu\left(\sphericalangle^{\pi^+}_{\pi^0}; M_\rho^2, M_\rho^2\right). \tag{34}$$

3.2.2 Universal confinement singularity

To write the amplitude with universal confinement interaction, we should change in (32) the t-channel confinement block: $(\hat{q}^{\perp})I_1^{(\mu\to 0)}(t_\perp)\,G_{q\bar{q}\to\pi\pi}(t_\perp) \to (-)I_1^{(\mu\to 0)}(t_\perp)G_{q\bar{q}\to\pi\pi}(t_\perp)$. Therefore

$$A\left(\sphericalangle_{\pi^0}^{\pi^+};s,M_\rho^2\right)=\int\limits_{4m^2}^{\infty}\frac{ds'}{\pi}\Psi_\rho(s')d\Phi_2(p';k_1',k_2') \tag{35}$$

$$\times Sp\Big[(\hat{k}_1'+m)G_{q\bar{q}\to\pi\pi}(t_\perp)I_1^{(\mu\to 0)}(t_\perp)(-k_2'+m)\gamma_\nu^{\perp p'}\Big]\frac{p_{\pi^+\nu}^{\perp p}}{(p_{\pi^+\nu'}^{\perp p})^2}$$

$$=\int\limits_{4m^2}^{\infty}\frac{ds'}{\pi}\Psi_\rho(s')d\Phi_2(p';k_1',k_2')G_{q\bar{q}\to\pi\pi}(t_\perp)I_1^{(\mu\to 0)}(t_\perp)\left[8mz'\frac{\sqrt{s'/4-m^2}}{\sqrt{s/4-M_\pi^2}}\right].$$

In the right-hand side of (35) we put, as previously, $G_{q\bar{q}\to\pi\pi}(t_\perp)=G_{q\bar{q}\to\pi\pi}(0)+G_{q\bar{q}\to\pi\pi}(1)\,t_\perp+G_{q\bar{q}\to\pi\pi}(2)t_\perp^2$.

3.3 Estimation of confinement interaction couplings $G_{q\bar{q}\to\pi\pi}(n)$

Taking into account both the bremsstrahlung type and the direct confinement interaction transitions, the width of the $\rho\to\pi\pi$ decay is determined as follows:

$$M_\rho\Gamma_{\rho\to\pi\pi} = \int d\Phi_2(p;p_{\pi^0},p_{\pi^+})\frac{1}{3}\sum_\nu\left|A_\nu^{\rho^+\to\pi^+\pi^0}(\text{emission})+\text{A}_\nu^{\rho^+\to\pi^+\pi^0}(\text{direct transition})\right|^2$$

$$= \frac{1}{3}\frac{1}{16\pi}\sqrt{1-\frac{4M_\pi^2}{M_\rho^2}}\left(\frac{M_\rho^2}{4}-M_\pi^2\right)\left|4A\left(\triangle_{\pi^0}^{\pi^+};M_\rho^2,M_\rho^2\right)+2A\left(\sphericalangle_{\pi^0}^{\pi^+};M_\rho^2,M_\rho^2\right)\right|^2 \tag{36}$$

The factor $1/3$ is the consequence of averaging over the ρ meson spin. Let us recall that here $p^2=M_\rho^2$ and $|p_{\pi^+\nu}^{\perp p}|^2=M_\rho^2/4-M_\pi^2$.

3.3.1 Order of values of $G_{q\bar{q}\to\pi\pi}(1-N)$ at $N=0,1$

To estimate the order of values of $G_{q\bar{q}\to\pi\pi}(1-N)$ in (21) and (23), we fit the ρ-meson width ($\Gamma_{\rho\to\pi\pi}=150$ MeV) which is defined according Eq. (36), using one non-zero coupling $G_{q\bar{q}\to\pi\pi}(1-N)$ only. Each value of g_π results in two values of $G_{q\bar{q}\to\pi\pi}(1-N)$ because of the constructive and destructive interferences of $4A\left(\triangle_{\pi^0}^{\pi^+};M_\rho^2,M_\rho^2\right)$ and $2A\left(\sphericalangle_{\pi^0}^{\pi^+};M_\rho^2,M_\rho^2\right)$ in (36). We obtain for the Gribov quark-exchange and for the universal interactions the following couplings (in GeV units).

(i) Gribov quark-exchange interaction:

g_π	$G_{q\bar{q}\to\pi\pi}(0)$, $N=1$	$G_{q\bar{q}\to\pi\pi}(1)$, $N=0$
-2.96	(0.016 or 0.112)	0
16.85	(-0.411 or -0.315)	0
-2.96	0	(0.076 or 0.532)
16.85	0	(-1.957 or -1.501)

(37)

(ii) Universal confinement singularity:

g_π	$G_{q\bar{q}\to\pi\pi}(0)$, $N=1$	$G_{q\bar{q}\to\pi\pi}(1)$, $N=0$
-2.96	(0.007 or 0.047)	0
16.85	(-0.172 or -0.132)	0
-2.96	0	(0.112 or 0.784)
16.85	0	(-2.886 or -2.213)

(38)

4 Self-energy part in the $\rho \to \pi\pi \to \rho$ transition

In [5] we have calculated the levels and wave functions of states in the infinite wall approach (the requirement $\mu \to 0$ in Eq. (2)). Generally speaking, this means that in the width calculated according to Eq. (36) we neglect the reverse influence of the $\pi\pi$ channel on the characteristics of the ρ-meson. This is not a bad approximation for the ρ-meson, but in our consideration we can make the next step – to take into account the $\pi\pi$ channel – easily. This two-component equation is shown in a graphical form in Fig. 10: one component refers to the $(\rho \to q\bar{q})$-vertex, the second one to the $(\rho \to \pi\pi)$-vertex. The interaction block $q\bar{q} \to \pi\pi$ is deciphered in Fig. 11: it contains transitions considered in Chapters 2 and 3.

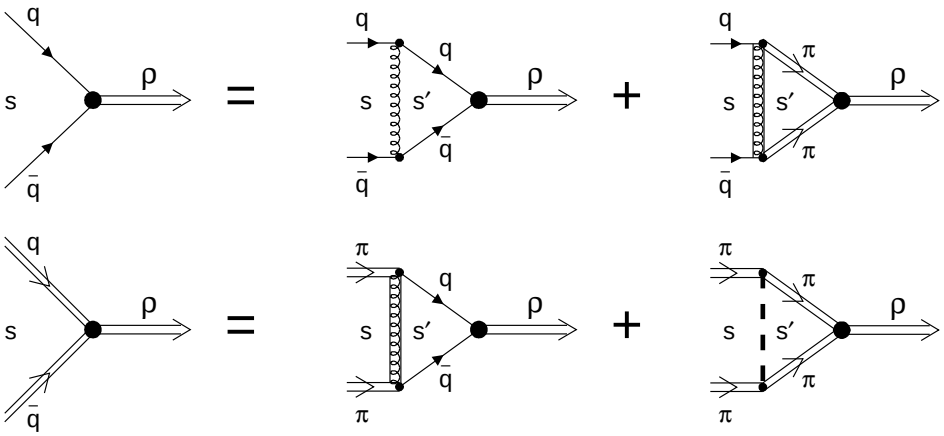

Figure 10: Graphical representation of two-channel $(q\bar{q}, \pi\pi)$ equations for the ρ-meson.

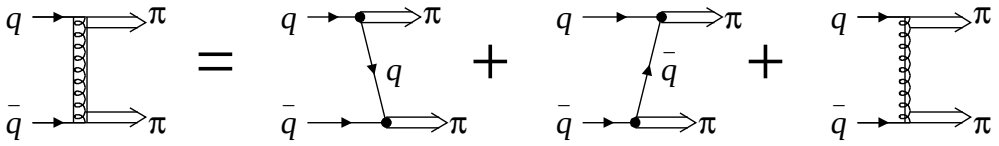

Figure 11: Three terms of the transition amplitude $q\bar{q} \to \pi\pi$.

Two simplifying constraints should be taken into account:
(i) the $\pi\pi$ interaction in the ρ-meson region is small,
(ii) the ρ-meson width is not large.

Then we have a standard one-channel equation for $\rho_{(q\bar{q})}$, where $\rho_{(q\bar{q})}$ is a pure $q\bar{q}$-state, see Fig. 12a, while the $\pi\pi$ channel reveals itself in the self-energy part of transition $\rho_{(q\bar{q})} \to \pi\pi \to \rho_{(q\bar{q})}$ only, see Fig. 12b. We denote this self-energy part as $B(s, M^2_{\rho(q\bar{q})})$ with the initial and final state energy squared $M^2_{\rho(q\bar{q})}$ and s.

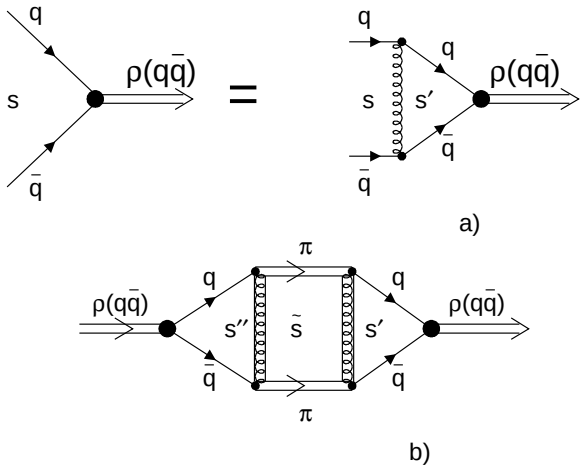

Figure 12: Graphical representation of a) the equation for the pure $q\bar{q}$ state $\rho(q\bar{q})$ and b) the self-energy part $B(s, M^2_{\rho(q\bar{q})})$ which determines the admixture of the $\pi\pi$ component in the ρ-meson according to Eq. (39).

The propagator of the pure $q\bar{q}$-state is transformed as follows:

$$\begin{aligned} \frac{\sum\limits_a \epsilon^{(a)}_\nu \epsilon^{(a)+}_{\nu'}}{M^2_{\rho(q\bar{q})} - s} \;&\to\; \frac{\sum\limits_a \epsilon^{(a)}_\nu \epsilon^{(a)+}_{\nu'}}{M^2_{\rho(q\bar{q})} - s - B(s, M^2_{\rho(q\bar{q})})} \\ &= \frac{\sum\limits_a \epsilon^{(a)}_\nu \epsilon^{(a)+}_{\nu'}}{\Big(M^2_{\rho(q\bar{q})} - \mathrm{Re}B(s, M^2_{\rho(q\bar{q})})\Big) - s - i\,\mathrm{Im}B(s, M^2_{\rho(q\bar{q})})}\,. \end{aligned} \tag{39}$$

The pole requirement reads

$$M^2_{\rho(q\bar{q})} - \mathrm{Re}B(s, M^2_{\rho(q\bar{q})}) - s = 0 \quad \text{at} \quad s = M^2_\rho \equiv (0.775)^2\,\mathrm{GeV}^2. \tag{40}$$

Then the width Γ_ρ is equal to:

$$\mathrm{Im}B(M^2_\rho, M^2_{\rho(q\bar{q})}) = M_\rho \Gamma_\rho\,. \tag{41}$$

From the results of the fit [5] we know that $M^2_\rho = M^2_{\rho(q\bar{q})}$, *i.e.* the fit provides us with a negligibly small value of the mass shift. So, we may accept:

$$\mathrm{Re}\,B(M^2_\rho, M^2_{\rho(q\bar{q})}) = 0. \tag{42}$$

4.0.2 Self-energy part $B(s, M^2_{\rho(q\bar{q})})$

The self-energy part of a pure $q\bar{q}$-state reads

$$B(s, M^2_{\rho(q\bar{q})}) = \int\limits_{4M^2_\pi}^{\infty} \frac{d\tilde{s}}{\pi} \frac{\mathrm{Im}B(\tilde{s}, M^2_{\rho(q\bar{q})})}{\tilde{s} - s - i0}, \tag{43}$$

where

$$\mathrm{Im}B(s,M^2_{\rho(q\bar{q})})=\frac{1}{192\pi}\sqrt{\frac{(s-4M_\pi^2)^3}{s}}\Big(4A\left(\triangle^{\pi^+}_{\pi^0};s,M^2_\rho\right)+2A\left(\triangleleft^{\pi^+}_{\pi^0};s,M^2_\rho\right)\Big)^2. \qquad (44)$$

Here we take into account that the amplitudes $A\left(\triangle^{\pi^+}_{\pi^0};s,M^2_\rho\right)$ and $A\left(\triangleleft^{\pi^+}_{\pi^0};s,M^2_\rho\right)$ do not have imaginary parts in the $\mu\to 0$ limit despite of the fact that $q\bar{q}$ is present in their intermediate states, see Fig. 6 and Eqs. (7), (32), (35). This means non-flying out quarks in the resonance decay, *i.e.* quark confinement. The only particles flying out are pions; this fact manifests itself in the presence of the threshold singularity in (43) at $s=4M_\pi^2$.

The requirement $M^2_\rho=M^2_{\rho(q\bar{q})}$ given in Eq. (42) reads:

$$\mathrm{P}\int\limits_{4M_\pi^2}^{\infty}\frac{d\tilde{s}}{\pi}\frac{\mathrm{Im}B(\tilde{s},M^2_{\rho(q\bar{q})})}{\tilde{s}-M^2_{\rho(q\bar{q})}}=0, \qquad (45)$$

here P means the principal value of the integral.

It is natural to think that the requirement (45) is realized by the behaviour of $\mathrm{Im}B(\tilde{s},M^2_{\rho(q\bar{q})})$ at large $\tilde{s}$ but not in the region $\tilde{s}\sim M^2_{\rho(q\bar{q})}$. The region of large $\tilde{s}$ is, however, beyond our present considerations. We could try to produce the condition (42) staying in the framework of our calculations (by, *e.g.*, choosing the couplings for $G_{q\bar{q}\to\pi\pi}(0)$, $G_{q\bar{q}\to\pi\pi}(1)$, $G_{q\bar{q}\to\pi\pi}(2)$, or by introducing a cut-off, or by combining these methods). These would be, however, artificial procedures, not corresponding to the real formation mechanism of the self-energy part. Hence, we will not consider this possibility.

5 Conclusion

In the quark model the decay of a $q\bar{q}$ state into pions (*i.e.* when the quarks fly out of their "trap") is described by processes shown in Fig. 6. Let us underline that, from the point of view of a quantum mechanical or a dispersion description, where time ordering exists, these are different processes – not so in the Feynman diagram ideology which does not include time ordering. We consider the problem in the framework of the dispersion technics approach.

Our investigations show that the bremsstrahlung-type radiation of pions (*i.e.* radiation coming from the region of the confinement trap) is rather large. If this were the only possible process, it would lead to a very broad decay width of the ρ-meson, $\sim$ 2000 MeV. But the process which involves the Gribov singularity, Fig 6, prevents such a "smearing" and we see quite a number of relatively narrow $q\bar{q}$ states.

Let us note that this is not the only process leading to narrow $q\bar{q}$ states. The accumulation of widths of highly excited $q\bar{q}$-resonances by their exotic neighbours (*e.g.* by glueballs, see [1] – Chapter 2 and references therein) leads to a similar effect of keeping the quarks inside the trap. But, and this is important to underline, such an accumulation of widths can take place only in those regions and for those states where exotic neighbours exist, while the process with Gribov singularities is always possible, *i.e.* it is universal.

The Gribov singularities are not determined unambiguously from the investigation of the $\rho(775)\to\pi\pi$ decay. Their determination is, apparently, possible, but this requires a much more complete knowledge of the $\pi\pi$ decays.

Quark confinement, *i.e.* the absence of $q\bar{q}$-singularities in hadron amplitudes when there are $q\bar{q}$-systems in the intermediate states is owing to interactions shown in Fig. 8a and Fig. 8b. But the physics of $q\bar{q}$-resonances has to deal also with the interactions in Fig. 8c. Indeed, the interactions Fig. 8a and Fig. 8b guarantee the confinement of quarks (at $\mu \to 0$), but can not prevent a very fast decay, a "smearing" of a $q\bar{q}$-system.

References

[1] A.V. Anisovich, V.V. Anisovich, M.A. Matveev, V.A. Nikonov, J. Nyiri and A.V. Sarantsev, *Mesons and Baryons*, World Scientific, Singapore (2008).

[2] A.V. Anisovich, V.V. Anisovich, V.N. Markov, V.A. Nikonov, and A.V. Sarantsev, Yad. Fiz. **68**, 1614 (2005) [Phys. At. Nucl. **68**, 1554 (2005)]; hep-ph/0401224.

[3] V.V. Anisovich, L.G. Dakhno, M.A. Matveev, V.A. Nikonov, and A. V. Sarantsev, Yad. Fiz. **70**, 68 (2007) [Phys. Atom. Nucl. **70**, 63 (2007)]; hep-ph/0510410.

[4] V.V. Anisovich, L.G. Dakhno, M.A. Matveev, V.A. Nikonov, and A.V. Sarantsev, Yad. Fiz. **70**, 392 (2007) [Phys. Atom. Nucl. **70**, 364 (2007)]; hep-ph/0511105.

[5] V.V. Anisovich, L.G. Dakhno, M.A. Matveev, V.A. Nikonov, and A. V. Sarantsev, Yad. Fiz. **70**, 480 (2007) [Phys. Atom. Nucl. **70**, 450 (2007)]; hep-ph/0511109.

[6] A.V. Anisovich, V.V. Anisovich, and A.V. Sarantsev, Phys. Rev. D **62**, 051502(R) (2000).

[7] L.G. Dakhno, V.A. Nikonov, Eur. Phys. J. A5, 209 (1999);
L.G. Dakhno, in "Frontiers in Strong Interactions", Proceedings of VI Blois Workshop, p.189, eds. P. Chiappetta, M. Hagenauer, J. Tran Thanh Van, Edition Frontière, Gif-sur-Yvette (1995).

[8] H. Satz, Phys. Lett. **B**25, 220 (1967).

[9] V.V. Anisovich '*Strong Interaction in High Energies and the Quark-Parton Model*' in Proc. of the IX LNPI Winter School, v.3, p.106, ed. Y.N. Novikov, Leningrad (1974).

[10] A. Capella *et al.*, Phys. Lett. **81**, 68 (1979).

[11] V.N. Gribov, '*The Gribov Theory of Quark Confinement*', World Scientific, Singapore (2001).

[12] A.V. Anisovich, V.V. Anisovich, L.G. Dakhno, M.A. Matveev, V.A. Nikonov, and A. V. Sarantsev '*The $\rho \to \gamma\pi$ and $\omega \to \gamma\pi$ Decays in Quark-Model Approach and Estimation of Coupling for Pion Emission by Quark*', hep-ph/0901.4854v1.

[13] V. Stoks, R. Timmermans, J.J. de Swart, Phys. Rev. C **47**, 512 (1993).

[14] R.A. Arndt, I.I. Strakovsky and R.L. Workman, Phys. Rev. C **50**, 2731 (1994); ArXiv:nucl-th/9506005.

[15] D.V. Bugg, R. Marchleidt, '*πNN coupling constant from NN elastic data between 210 800 MeV*', preprint NUCL-TH-9404017 (1994).